Spectrally selective optical pumping in Doppler-broadened cesium atoms*

Zhang Jun-Hai(张军海)†, Zeng Xian-Jin(曾宪金), Li Qing-Meng(李庆萌), Huang Qiang(黄 强), and Sun Wei-Min(孙伟民)

Science School, Harbin Engineering University, Harbin 150001, *China*

(Received 27 September 2012; revised manuscript received 23 October 2012)

The D_1 line spectrally selective pumping process in Doppler-broadened cesium is analyzed by solving the optical Bloch equations. The process, described by a three-level model with the Λ scheme, shows that the saturation intensity of broadened atoms is three orders of magnitude larger than that of resting atoms. The $|F_g = 3\rangle \rightarrow |F_e = 4\rangle$ resonance pumping can result in the ground state $|F_g = 4, m_F = 4\rangle$ sublevel having a maximum population of 0.157 and the population difference would be about 0.01 in two adjacent magnetic sublevels of the hyperfine (HF) state $F_g = 4$. To enhance the anisotropy in the ground state, we suggest employing dichromatic optical HF pumping by adding a laser to excite D_1 line $|F_g = 4\rangle \rightarrow |F_e = 3\rangle$ transition, in which the cesium magnetometer sensitivity increases by half a magnitude and is unaffected by the nonlinear Zeeman effect even in Earth's average magnetic field.

Keywords: spectrally selective pumping, hyperfine structure, population

PACS: 32.80.Xx, 32.10.–f, 32.30.–r **DOI:** 10.1088/1674-1056/22/5/053202

1. Introduction

Spectrally selective pumping is a useful way to obtain an anisotropic medium and has important applications in high-precision measurement, such as atomic clocks,[1,2] laser spectroscopy, atomic filters,[3] and atomic magnetometers.[4,5] So optically pumped processes have been researched by many scientists, both theoretically and experimentally, in recent years. Several contrasting methods are proposed to calculate and analyze the time evolution of optically pumped alkali-metal atoms, including rate equations,[6,7] density matrix formalisms,[8,9] and quantum electrodynamics.[10] These theories can get identical results after a few microseconds of interaction, even though they have different formal differential equations. From the experimental point of view, cesium has become an excellent candidate for developing atomic magnetometers recently, since it has the highest saturation vapor pressure and the largest hyperfine HF splitting in the ground state of all alkali metals, although it has the most complicated structure in the HF sublevels.

The present paper discusses the Cs D_1 line selective pumping processes, characterized by a model with a Λ three-level atom structure, and then points out that the saturation intensity of a left-hand circularly polarized (σ^+) laser with the $F_g = 3 \rightarrow F_e = 4$ resonant frequency is about 1.46 mW/cm^2 in Doppler-broaden atoms, theoretically. To investigate the dependence of the anisotropy in the ground state on a pumping laser, we analyze the time evolution of the correlative HF magnetic sublevels by solving rate equations and indicate that the $|F_g = 4,\ m_F = 4\rangle$ sublevel should have a maximum population of 0.157 and the population difference between adjacent sublevels in ground state $F_g = 4$ would be about 0.01 after becoming steady. On the basis of the analysis, we propose a new all-optical cesium magnetometer using dichromatic optical HF pumping, which can increase the resonance magnitude by one order of magnitude compared to the traditional optically pumped magnetometer with a single mode laser, and simultaneously eliminate the nonlinear Zeeman effect on sensitivity in a terrestrial magnetic field.

2. Pumping process and analysis

The D_1 line HF structure of Cs is shown in Fig. 1(a). The HF splitting frequency in the ground state is 9.2 GHz, which is much larger than 400 MHz Doppler width at room temperature, so while a σ^+ laser with $F_g = 3 \rightarrow F_e = 4$ resonance depletes the population of the $F_g = 3$ state (as shown in Fig. 1(a)), the $F_g = 4$ level should become a leaky trapped state and its population should increase due to the repopulation from the excited state, thus the pumping process might be taken into account in an atomic model with a Λ structure, as shown in Fig. 1(b).

We confirm the saturation intensity in the scheme theoretically, and write the optical Bloch equations as

$$\dot{\rho}_{aa} = -\frac{i}{2}\Omega_p(\rho_{ab} - \rho_{ba}) + \Gamma_{ba}\rho_{bb} + \gamma(\rho_{cc} - \rho_{aa}), \quad (1)$$

$$\dot{\rho}_{ab} = \frac{i}{2}\Omega_p(\rho_{bb} - \rho_{aa}) - i\left(\Delta + \frac{\Gamma_{ba}}{2}\right)\rho_{ab}, \quad (2)$$

*Project supported by the International Cooperation Project of the Ministry of Science and Technology of China (Grant No. 2008DFR20420) and the Fundamental Research Funds for the Central Universities, China (Grant No. HEUCF20111111).

†Corresponding author. E-mail: jhzhang@hrbeu.edu.cn

© 2013 Chinese Physical Society and IOP Publishing Ltd

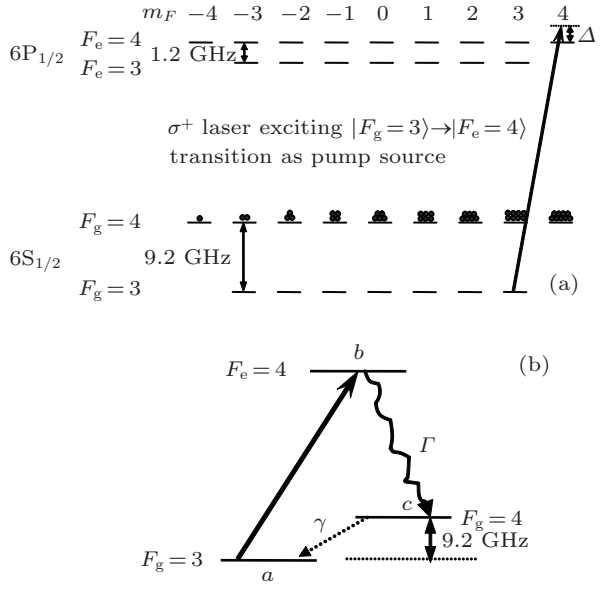


Fig. 1. (a) Cesium HF structure of Cs D_1 line transition. (b) Equivalent model of spectrally selective HF pumping in Cs.

$$\dot{\rho}_{bb} = \frac{i}{2}\Omega_p(\rho_{ab} - \rho_{ba}) - \Gamma\rho_{bb}, \tag{3}$$

$$\dot{\rho}_{cc} = \Gamma_{bc}\rho_{bb} - \gamma(\rho_{cc} - \rho_{aa}). \tag{4}$$

Here, ρ_{aa}, ρ_{cc}, and ρ_{bb} are populations of the ground states $F_g = 3$, $F_g = 4$, and excited state $F_e = 4$, so $\rho_{aa}+\rho_{bb}+\rho_{cc} = 1$, Γ is the natural decay rate of $F_e = 4$, and Γ_{ba} and Γ_{bc} represent the spontaneous emission rates from the excited state to both the ground states, and thus $\Gamma = \Gamma_{ba} + \Gamma_{bc}$, $\gamma \ll \Gamma$ is the relaxation rate between the ground states, Δ and $\Omega_p = \mu E/\hbar^2$ denote the frequency detuning and the Rabi frequency of the pump light, where μ, E, and $\hbar$ are the dipole moment operator, the electric field amplitude, and the Planck constant, respectively. Solving Eqs. (1)–(4), one can define the optical intensity as the saturation intensity while the population of $F_g = 3$ is reduced to the half of the initial value, and then obtain

$$I_{sat} = \frac{c\varepsilon_0\hbar^2}{\mu^2}\left(1 + \frac{4\Delta^2}{\Gamma^2}\right)\Gamma\gamma. \tag{5}$$

Here, c and ε_0 represent the speed of light and the permittivity of vacuum. The optical intensity $I = c\varepsilon_0 E^2/2$ is taken into account here. This demonstrates that the relaxation between both the ground states results in the atom having factor γ/Γ saturation intensity compared to an atom with a two-level structure.[3] Whereas because of the thermal velocity of an atom moving along the pumping direction in a Cs cell, the velocity distribution in that direction has to be considered in the calculation, and then the expression can be rewritten as

$$I'_{sat} = \frac{c\varepsilon_0\hbar^2\Gamma\gamma}{\mu^2}\frac{1}{u\sqrt{\pi}}\int_{-\infty}^{+\infty}\left(1 + \frac{4(\Delta + \boldsymbol{k}\cdot\boldsymbol{v})^2}{\Gamma^2}\right)e^{-v^2/u^2}\,d\boldsymbol{v}. \tag{6}$$

Here, u is the probable velocity of atoms, $\boldsymbol{k}$ is the wave vector of the pump light, $\boldsymbol{v}$ denotes the moving velocity of the atom. To compare the expressions quantitatively, we assume $\gamma/\Gamma = 10^{-4}$[11] and plot saturation intensities of the pump beam as a function of the frequency detuning together in Fig. 2. The figure displays explicitly that the resting atom has a saturation intensity of about 0.3 μW/cm^2 on resonance only because the slow relaxation makes the saturation intensity decrease by several orders of magnitude in comparison to a two-level atom,[3] while for the moving atom, there is a resonant saturation intensity of 1.46 mW/cm^2. This means that normally a single mode extended cavity diode laser can easily provide saturation intensity for the circular polarization pumping with the D_1 resonance that is an order of magnitude greater, as has been shown experimentally.[4,12] If the detuning of a pump laser is over 0.7 GHz, the two cases have the same saturation intensity, as shown in Fig. 2, because almost all of the atoms see the light as being the same frequency under this condition.

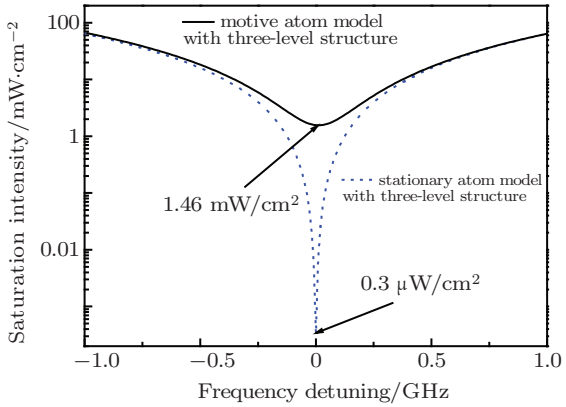


Fig. 2. (color online) Saturation intensity of the D_1 line σ^+ transition from $F_g = 3$ to $F_e = 4$ as a function of the pump's frequency detuning in two cases: dotted and solid curves represent the static and moving atom models with a three-level Λ scheme.

In order to understand how resonant circular polarization pumping would cause cesium vapor to become anisotropic, it is necessary to calculate the dynamic population evolvement in each HF magnetic sublevel of ground and excited states. Considering an anti-relaxation coated cell containing the cesium vapor with number density of 10^{11} cm^{-3} in the experiment,[13] we can ignore atomic perturbation probability due to atom-atom collisions in the excited state. When a pump laser has σ^+ polarization (as shown in Fig. 1(a)), the populations of the magnetic sublevels of the ground and excited states are expressed by rate equations, and the results are as follows:

$$\begin{aligned}\frac{d\boldsymbol{P}_{F_g=3,m_F}}{dt} &= -\boldsymbol{R}^{F_e=4,m_F+1}_{F_g=3,m_F}\frac{\Gamma}{2}\frac{I}{I_{sat}}\frac{(\boldsymbol{P}_{F_g=3,m_F} - \boldsymbol{Q}_{F_e=4,m_F})}{1+4(\Delta+\boldsymbol{k}\cdot\boldsymbol{v})^2/\Gamma^2} \\ &+ \sum_{m'_F=m_F-1}^{m'_F=m_F+1}\boldsymbol{R}^{F_e=4,m'_F}_{F_g=3,m_F}\Gamma\boldsymbol{Q}_{F_e=4,m'_F} \\ &+ \sum_{m'_F\neq m_F}\gamma(\boldsymbol{P}_{F_g=3,m'_F} - \boldsymbol{P}_{F_g=3,m_F}) \\ &+ \sum_{m'_F=-4}^{m'_F=4}\gamma(\boldsymbol{P}_{F_g=4,m'_F} - \boldsymbol{P}_{F_g=3,m_F}),\end{aligned} \tag{7}$$

$$\frac{\mathrm{d}\boldsymbol{P}_{F_g=4,m_F}}{\mathrm{d}t} = \sum_{m'_F=m_{F_g}-1}^{m'_F=m_{F_g}+1} \boldsymbol{R}^{F_e=4,m'_F}_{F_g=4,m_{F_g}} \Gamma \boldsymbol{Q}_{F_e=4,m'_F} + \sum_{m'_F\neq m_F} \gamma(\boldsymbol{P}_{F_g=4,m'_F} - \boldsymbol{P}_{F_g=4,m_F}) + \sum_{m'_F=-3}^{m'_F=3} \gamma(\boldsymbol{P}_{F_g=3,m'_F} - \boldsymbol{P}_{F_g=4,m_F}), \quad (8)$$

$$\frac{\mathrm{d}\boldsymbol{Q}_{F_e=4,m_F}}{\mathrm{d}t} = C^{F_e=4,m_F}_{F_g=3,m_F-1} \frac{\Gamma}{2}\frac{I}{I_{\mathrm{sat}}} \frac{(\boldsymbol{P}_{F_g=3,m_F-1} - \boldsymbol{Q}_{F_e=4,m_F})}{1+4(\Delta+\boldsymbol{k}\cdot\boldsymbol{v})^2/\Gamma^2} - \sum_{m'_F=m_F-1}^{m'_F=m_F+1} \boldsymbol{R}^{F_e=4,m_F}_{F_g=3,m'_F} \Gamma \boldsymbol{Q}_{F_e=4,m_F} - \sum_{m'_F=m_F-1}^{m'_F=m_F+1} \boldsymbol{R}^{F_e=4,m_F}_{F_g=4,m'_F} \Gamma \boldsymbol{Q}_{F_e=4,m_F}. \quad (9)$$

Here, $\boldsymbol{P}_{F_g,m_F}$ and $\boldsymbol{Q}_{F_e,m_F}$ represent the populations of the ground state sublevel $|F_g,\ m_F\rangle$ and the excited state $|F_e,\ m_F\rangle$ respectively; $\boldsymbol{R}^{F_e=4,m_F}_{F_g,m'_F}$ is the normalized transition strength between sublevels $|F_g,\ m'_F\rangle$ and $|F_e=4,\ m_F\rangle$.[3] In the calculation, the HF sublevel shifts and relaxation induced by the magnetic field to be measured are ignored completely, because they are smaller in comparison with the natural width of the excited state (about 4.6 MHz). The above analysis is correct for an atom with specified velocity. In view of the atomic thermal velocity, likewise, it is necessary to revise populations in the $F_g=3$ and $F_e=4$ Zeeman sublevels, and these results are given by the following expressions

$$\boldsymbol{P}'_{F_g=3,m_{F_g}} = \frac{1}{u\sqrt{\pi}} \int_{-\infty}^{+\infty} \boldsymbol{P}_{F=3,m_{F_g}} (\Delta+\boldsymbol{k}\cdot\boldsymbol{v})\, \mathrm{e}^{-\boldsymbol{v}^2/u^2}\, \mathrm{d}\boldsymbol{v}, \quad (10)$$

$$\boldsymbol{Q}'_{F_e=4,m_{F_e}} = \frac{1}{u\sqrt{\pi}} \int_{-\infty}^{+\infty} \boldsymbol{Q}_{F_e=4,m_{F_e}} (\Delta+\boldsymbol{k}\cdot\boldsymbol{v})\, \mathrm{e}^{-\boldsymbol{v}^2/u^2}\, \mathrm{d}\boldsymbol{v}. \quad (11)$$

Based on practical experimental conditions, we assume that the σ^+ pump laser, having a several megahertz line width and $I=4I'_{\mathrm{sat}}$ intensity, is tuned to the D_1 $F_g=3\rightarrow F_e=4$ transition. The intensity should cause a population relaxation time of hundreds of nanoseconds (ns), which is enough for geomagnetic field measurement, even though increasing the intensity can shorten the time.[7] Solving Eqs. (7)–(11), one can obtain the numerical solutions of the population dynamics of every correlative sublevel; and the results are shown in Fig. 3.

Figure 3(a) shows clearly that the populations of the $F_g=3$ sublevels decrease rapidly with increasing interactive time, then finally reach zero. Figure 3(b) reveals the time evolution of the populations of the $F_e=4$ sublevels According to the selection rules, the populations of $|F_e=4,\ m_F=-4\rangle$ and $|F_e=4,\ m_F=-3\rangle$ are not affected by the pumping process and always remains zero; the populations of the rest of the $F_e=4$ sublevels have an initial increase and attain the peak value of a few percent after several nanoseconds,

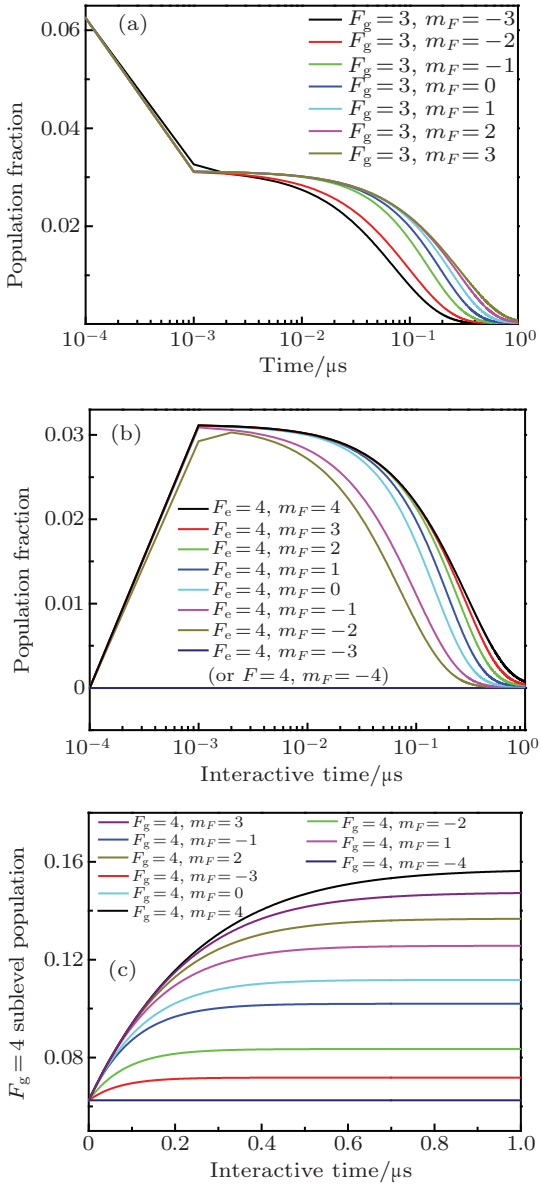


Fig. 3. Time evolution of the magnetic sublevel populations of three HF components after turning the pump light on: (a) $F_g=3$, (b) $F_e=4$, (c) $F_g=4$.

and then decline and ultimately reach zero as well, as expected. Figure 3(c) interprets the formation process of the anisotropic medium: all the $F_g=4$ magnetic sublevels had equal populations of 1/16 at the initial time, except that the state $|F_g=4,\ m_F=-4\rangle$ populations of each sublevel increase gradually via spontaneous emission from the excited state $F_e=4$, and then after hundreds of nanoseconds of interaction they almost become steady. In this case, the population increases continually with the magnetic quantum number (as shown in Fig. 1(a)), so $|F_g=4,\ m_F=4\rangle$ might have a maximum population of about 0.157, and the population difference between adjacent sublevels would be about 0.01. On the other hand, it has been discussed that the population of nine sublevels in the ground state $F_g=4$ varies with the pumping light intensity (see Fig. 4) when the interactive time among light and atoms is quite long (about microsecond magnitude).

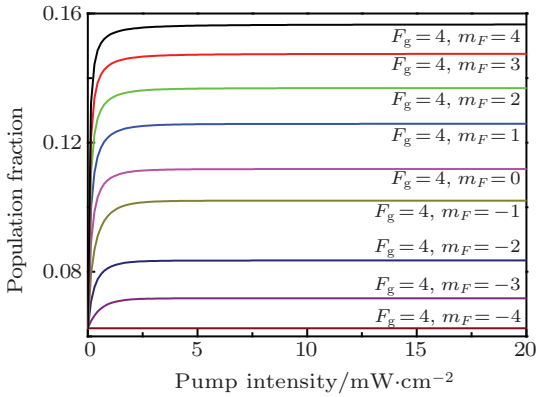


Fig. 4. Populations of the $F_g = 4$ Zeeman sublevels as a function of the pump intensity.

The result explains that after the pump intensity reaches 6 mW/cm^2 (about 4 times of the saturation intensity), further increasing the intensity will not alter the populations of the $F_g = 4$ magnetic sublevels, and will not affect the vapor anisotropy, because all the $F_g = 3$ sublevels become empty at this intensity.

3. Discussion

Our designed magnetometer measures the strength of the external magnetic field based on the magnetic resonance in $F_g = 4$ sublevels,[12] so the device sensitivity depends on the spectral figure of merit and the system noise. Since the experiment adopted the optical structure in which the transmission direction of the probe laser is orthogonal to that of the pump light, noises derived from frequency and intensity fluctuations of the pump beam cannot be found by the detector and are neglected. In a weak field (≤ 2 μT) condition where the nonlinear Zeeman shift in the ground state can be neglected, eight resonant spectrum components from the nine magnetic sublevels have the same resonant frequency and linewidth. Therefore, measured signal magnitude, which is proportional to the population difference between $|F_g = 4,\ m_F = 4\rangle$ and $|F_g = 4,\ m_F = -4\rangle$, is about 0.1, and its width would be 20 Hz.[12] However, in a geomagnetic field (about 50 μT), the quadratic Zeeman effect leads to a resonant frequency separation of 7 Hz between the adjacent magnetic sublevels. Therefore, not only do eight resonances practically blend into a single asymmetric contour with 50 Hz width at least, but also the corresponding amplitude decreases to some degrees. In order to overcome the intrinsic disadvantage of the pumping with a single mode diode laser here, we suggest preparing a pure quantum state $|F_g = 4,\ m_F = 4\rangle$ using dichromatic optical HF pumping, i.e., adding an assistant repump laser with the elliptical polarization, whose intensity can be about one third of the main laser and frequency is tuned to the D_1 line $|F_g = 4\rangle \rightarrow |F_e = 3\rangle$ transition avoiding evident intensity broadening and coherent population trap (CPT), as shown in Fig. 5. In this way, except for the state $|F_g = 4,\ m_F = 4\rangle$, Hence, all other ground state Zeeman sublevels will have no population. So the resonant amplitude will increase nearly one order of magnitude. It is particularly important that the spectrum width cannot be affected by the nonlinear Zeeman shift though the assistant light source. This might lead to a linewidth increase of up to 25% due to the relaxation induced by the repump laser,[13,14] which means that dichromatic pumping would enhance the figure of merit of the resonant signal by six to seven times. In fact, to minimize the optical frequency shift,[13] the detailed parameters of the assistant laser (for example intensity, frequency detuning, and elliptical degree) can be determined in experiment with the improved magnetometer, which will become our main research subject in the near future.

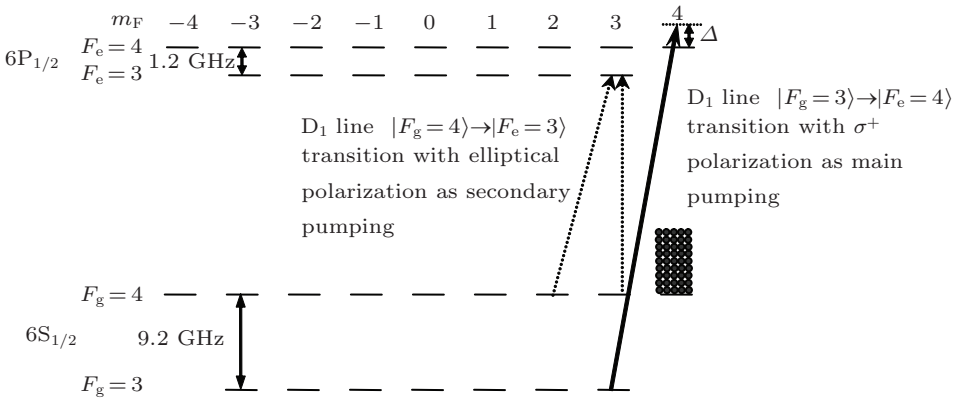


Fig. 5. Preparing the pure quantum state using dichromatic optical HF pumping.

4. Conclusion

In this paper, we analyzed the D_1 line spectrally selective pumping process in Doppler-broadened cesium, which is described by a three-level model with the Λ scheme, showing that the Doppler-broadened atom has much larger saturation intensity than the resting atom. While the atoms are pumped by a single mode laser with the D_1 line $|F_g = 3\rangle \rightarrow |F_e = 4\rangle$

resonant frequency and turn into an anisotropic medium, the ground state $|F_g = 4,\ m_F = 4\rangle$ sublevel can reach steady state with a maximum population of 0.157 and the population difference between adjacent Zeeman sublevels be about 0.01 in the HF component. In order to improve the anisotropy, we have proposed to add an HF repump laser exciting the D_1 line $|F_g = 4\rangle \rightarrow |F_e = 3\rangle$ resonance, which would be an effective approach to improve the sensitivity of the magnetometer by half a magnitude.

References

[1] Cheng H D, Wang X C, Xiao L, Zhang W Z, Liu L and Wang Y Z 2011 *Chin. Phys. B* **20** 023701

[2] Liu G B, Zhao F and Gu S H 2009 *Chin. Phys. B* **18** 3839

[3] Liu S Q, Zhang Y D, Fan D K, Wu H and Yuan P 2011 *Appl. Opt.* **50** 1620

[4] Ledbetter M P, Savukov I M, Acosta V M, Budker D and Romalis M V 2008 *Phys. Rev. A* **77** 033408

[5] Budker D, Kimball D F, Yashchuk V V and Zolotorev M 2002 *Phys. Rev. A* **65** 055403

[6] Moon G and Noh H R 2008 *J. Opt. Soc. Am. B* **25** 701

[7] Harris M L, Adams C S, Cornish S L, Mcleod I C, Tarleton T and Hughes I G 2006 *Phys. Rev. A* **73** 062509

[8] Zigdon T, Gordon A D W and Friedmann H 2008 *Phys. Rev. A* **77** 033836

[9] Li S J, Wang B, Yang X D, Han Y X, Wang H, Xiao M and Peng K C 2006 *Phys. Rev. A* **74** 033821

[10] Farrell P M, Gillivary W R M and Standage M C 1988 *Phys. Rev. A* **37** 4240

[11] Meshulam R, Zigdon T, Gordon A D W and Friedmann H 2007 *Opt. Lett.* **32** 2318

[12] Zhang J H, Liu Q, Zeng X J, Li J X and Sun W M 2012 *Chin. Phys. Lett.* **29** 068501

[13] Aleksandrov E B and Vershovskii A K 2009 *Physics-Uspekhi* **52** 573

[14] Groeger S, Bison G and Weis A 2005 *European Quantum Electronics Conference*, June 12–17, 2005, Munich, Germany, p. 199